Journal of Antivirals & Antiretrovirals
ISSN: 1948-5964

Alam et al., J Antivir Antiretrovir 2016, 8:4
DOI: 10.4172/1948-5964.1000147

Research Article Open Access

Verapamil has Antiviral Activities that Target Different Steps of the Influenza Virus Replication Cycle

Mohammad Intakhab Alam[1,2], Ahmed Mostafa[1,3], Pumaree Kanrai[1,4], Christin Müller[1], Julia Dzieciolowski[1,5], Eva Lenz[1], Irina Kuznetsova[1], Patricia Schult-Dietrich[6], John Ziebuhr[1], Ursula Dietrich[6] and Stephan Pleschka[1]*

[1]*Institute of Medical Virology, Justus-Liebig-University Giessen, Schubertstr. 81,35392 Giessen, Germany*
[2]*Department of Medical Microbiology, Emine-Bahaeddine Nakiboglu Medical School, Zirve University, Turkey*
[3]*Center of Scientific Excellence for Influenza Viruses, National Research Centre (NRC), Dokki, Giza, Egypt*
[4]*Department of Internal Medicine, University of Giessen & Marburg Lung Center, Graffkystraße 11, 35392, Germany*
[5]*Institute of Nutritional Science, Justus-Liebig-University Giessen, Heinrich-Buff-Ring 26-32, 35390 Giessen, Germany*
[6]*Georg-Speyer-Haus, Institute for Tumor Biology and Experimental Therapy, Paul- Ehrlich-Str. 42-44, 60596 Frankfurt, Germany*

Abstract

Safe and efficacious therapeutic options for infections caused by highly pathogenic influenza viruses (IV) remain limited. Viruses resistant to approved antiviral drugs are increasingly emerging and, in some cases, existing vaccines are insufficient to prevent seasonal epidemics or pandemics caused by these viruses. As a consequence, alternative antiviral strategies that, for example, target cellular factors or mechanisms essential for IV propagation have attracted increasing interest over the past years. Here, we characterized antiviral effects of the calcium channel blocker Verapamil on different steps of the IV replication cycle. Our data suggest that Verapamil (i) efficiently reduces influenza A and B virus titres in cell culture at non-toxic concentrations, (ii) does not influence virus entry, (iii) impairs the replication and transcription activity of the viral polymerase, (iv) decreases viral protein production, (v) reduces virus-induced NF-κB activation and (vi) does not induce the emergence of resistant IV variants, resulting in strongly reduced infectious particle formation.

Keywords: Influenza A virus; Calcium channel blocker; NF-κB; Nuclear RNP export; Viral RdRp activity

Introduction

Influenza A viruses (IAV) pose a major threat to public health worldwide, causing thousands of deaths and considerable economic damage due to seasonal epidemics occurring regularly. Both, the newly emerging H5N1 variants of highly pathogenic avian IV (HPAIV) and recent infections of humans with low pathogenic avian IV (LPAIV) of the H7N9 subtype, were shown to be associated with high fatality rates of about 60% and 35%, respectively, and may even have pandemic potential [1,2]. The major problem in fighting IAV is the high genetic variability of the virus, resulting in the rapid formation of variants that escape the pre-existing immunity against (previously or currently) circulating virus strains [3] and the emergence of variants resistant to antiviral agents [4]. As (all) viruses critically depend on host cell functions to complete their life cycles, some of these functions are thought to be suitable targets for antiviral strategies. This also includes intra-cellular signalling cascades, which are induced by a wide range of virus families, such as mitogen-activated protein kinase (MAPK) pathways, that have been the subject of multiple studies published over the past years [5-7].

In previous studies, we have shown that the Raf/MEK/ERK signalling cascade is essential for efficient production of progeny infectious IAV. Inhibition of this pathway impairs the nuclear export of IAV RNPs [8]. We also observed that IAV is unable to compensate functional effects resulting from a blockade of this particular cellular pathway, for example by acquiring specific mutations [9]. Inhibition of the signalling cascade was shown to reduce IAV replication both, *in vitro* and *in vivo*, further supporting its key role in IV replication [10,11]. Interestingly, the cascade is activated at least in part by viral HA protein accumulation and the signal is transmitted via the calcium-dependent PKC-alpha to Raf [12]. In line with this observation, the calcium channel blocker Verapamil was found to reduce ERK activation.

Verapamil blocks voltage-dependent calcium channels and is widely used in the treatment of hypertension, angina pectoris, cardiac arrhythmia and cluster headaches. The arrhythmic effects are used to control the ventricular rate and approval for clinical use by the U.S. Food and Drug Administration (FDA) dates back to 1982 [13].

The inhibitory effects of Verapamil on IAV propagation in cell culture have been described many years ago [14]. Based on the observation that chlorpromazine, a calmoduline-binding drug, also inhibited IAV replication, it was suggested that both drugs may interfere with calmoduline-dependent intra-cellular activities that are required for (late steps) of IAV replication or assembly. Nevertheless, the molecular basis for the observed effects remained elusive at the time. In an attempt to close this gap of knowledge between the previous observation and the current understanding of IAV replication we performed the present study and now provide evidence that Verapamil profoundly affects the replication and transcription activity of the viral RNA-dependent RNA polymerase (RdRp), resulting in reduced expression of viral proteins and, consequently, reduced production of virus progeny. Furthermore, we demonstrate that Verapamil interferes with the virus-induced activation of the transcription factor NF-κB, known to be involved in the expression of pro-apoptotic factors and subsequent apoptotic caspase-3 activation, the latter shown previously to promote viral RNP export [15,16]. Taken together, the data suggest that Verapamil has diverse effects on both virus and host cell functions that collectively result in strongly reduced IAV replication *in vitro*.

***Corresponding author:** Stephan Pleschka, Institute of Medical Virology, Schubert str 81, 35392 Giessen, Germany, Tel: 0049 (0)641-99-47750; Fax: 0049 (0)641-99-41209; E-mail: stephan.pleschka@viro.med.uni-giessen.de

Received November 23, 2016; **Accepted** December 02, 2016, 2016; **Published** December 15, 2016

Citation: Alam MI, Mostafa A, Kanrai P, Müller C, Dzieciolowski J, et al. (2016) Verapamil has Antiviral Activities that Target Different Steps of the Influenza Virus Replication Cycle. J Antivir Antiretrovir 8: 121-130. doi:10.4172/1948-5964.1000147

Material and Methods

Cells, plasmids, virus and infection

293T cells (human embryonic kidney cells), A549 cells (human alveolar epithelial cells) and MDCK-II cells (Madin-Darby canine kidney cells) were maintained in complete Dulbecco's modified Eagle's medium (DMEM, Gibco Life Technologies, UK) supplemented with 10% foetal calf serum (FCS) and antibiotics (100 U/ml penicillin, 0.1 mg/ml streptomycin) at 37°C in a humidified atmosphere with 5% CO_2.

The full-length cDNAs of HA, NA and M derived from influenza virus strain A/Thailand1 (Kan-1)/2004 (H5N1) and used for pseudovirus production were described previously [17].

Prior to infection, confluent cells were washed with phosphate-buffered saline containing 1 mM $MgCl_2$, 0.9 mM $CaCl_2$ (PBS^{++}) and were then incubated with the influenza virus strain A/Puerto Rico/8/34 (PR8, H1N1) at the indicated multiplicity of infection (MOI) in PBS/BA (PBS containing 0.2% bovine albumin (PAA, Germany), 1 mM $MgCl_2$, 0.9 mM $CaCl_2$, 100 U/ml penicillin, and 0.1 mg/ml streptomycin) for 1 h at room temperature (RT). The inoculum was aspirated and the cells were further incubated with DMEM/BA medium (DMEM containing 0.2 % BA and antibiotics) at 37°C, 5% CO_2.

Influenza virus titration (focus assay)

Virus titres were determined as described previously [18]. Briefly, MDCK-II cells were grown in 96-well plates overnight at 37°C, 5% CO_2 to about 90% confluence. Then, the cells were washed once with PBS++ and inoculated with 50 µl virus samples of 10 fold serial dilutions in PBS/BA (10^{-1} to 10^{-7}). The inoculum was aspirated, 150 µl Avicel medium (DMEM/BA, 1.25% Avicel®, FMC BioPolymer, Belgium) and 2 µg/ml trypsin was added, and cells were further incubated at 37°C, 5% CO_2 for 24 h. To detect single foci of virus-infected cells, the cells were fixed and permeabilized with 150 µl fixing solution (4% paraformaldehyde (PFA), Roth, Germany) and 1% Triton X-100 (Roth, Germany) in PBS^{++} and kept at 4°C for 1 h. Thereafter, the solution was discarded and cells were washed 3x with PBS^{++} / 0.05% Tween-20 (Roth, Germany). Next, the cells present in one well were incubated with 50 µl of primary antibody (mouse anti-influenza A virus nucleoprotein mAb, kindly provided by S. Ludwig, Münster) diluted 1:100 in PBS++ containing 3% BSA (PAN Biotech, Germany). After 1 h incubation at RT, the cells were washed 3x with PBS++, 0.05% Tween-20 and incubated for 1 h at RT with 50 µl secondary antibody (goat anti-mouse HRP-antibody, Santa Cruz, USA) diluted 1:1000 in PBS++ containing 3% BSA. Next, the cells were washed 3x with PBS++ containing 0.05% Tween-20 and incubated with 40 µl AEC (3-Amino-9-ethylcarbazole) staining solution (Santa Cruz, USA). Following incubation for 40 min at 37°C, the substrate solution was removed and cells were washed 2x with dH_2O to remove salts. To detect and quantify foci, the 96-well plates were scanned with a resolution of 1200 dpi using an Epson Perfection V500 Photo scanner (Epson, Japan) and analysed using Photoshop software (Adobe, USA). Results represent means (± SEM) from three independent experiments.

Antiviral compounds

Verapamil (LKT Laboratories, USA) was dissolved in sterile water. For treatment, Verapamil-containing medium was added 2 h post infection (p.i.) to avoid any effects on virus entry [12,19,20]. The MEK inhibitor U0126 (Taros GmbH, Germany) was dissolved at a stock concentration of 10 mM in DMSO (Roth, Germany). From this stock solution a serial dilution was prepared in DMEM/BA to obtain the desired effective U0126 concentration. For treatment, U0126-containing medium was added after virus adsorption.

MTT assay and CC_{50} determination

To determine the median cytotoxic concentration of the compounds at which 50% of the cells are still viable (CC_{50}) an MTT assay was performed [10]. Briefly, A549 cells were seeded in 96 well microtitre plates and were grown over night. Growth medium was replaced with DMEM/BA containing different concentrations of Verapamil (0.0, 0.1, 1.0, 10, 25, 50, 100, 250, 500, 1000 µM) and the cells (n=8) were further incubated at 37°C, 5% CO_2 for 24 h. Then the cells were washed with PBS^{++} and left to recover for 60 min in complete DMEM. This was displaced with MTT-media (complete DMEM containing 0.123 mg/ml of MTT-reagent (Thiazolyl Blue Tetrazolium Bromide, Sigma Aldrich, USA)) and incubated for 90 min at 37°C, 5% CO_2. After discarding the MTT-media the cells were fixed with 4% PFA (Roth, Germany) for 30 min and then left to air-dry for 10-15 min. The blue crystals were dissolved in 200 µl Isopropanol per well. Adsorption of the blue colour was measured at 492 nm by an ELISA-Reader (BioTek, Germany).

For the determination of the CC_{50}, MTT values of the cell culture supernatants were calculated in percentage. The MTT value of the untreated control was set as 100% and the MTT values of Verapamil-treated samples were calculated as follows: Percentage viability=100/(MTT value of untreated sample x MTT value of inhibitor treated sample). The CC_{50} value (i.e. the concentration of Verapamil required to reduce the viability to 50%) was determined using "GraphPad Prism" version 6.00 software for iOS (GraphPad Software, USA) by plotting the percentage of viability as a function of the Verapamil concentration.

EC_{50} determination

To determine the effective concentration at which virus titres are reduced by 50% (EC_{50}), A549 cells were grown over night on 24-well plates at 37°C / 5% CO_2. Cells were then washed with PBS++ and infected with 100 µl of PR8 (MOI=3) or influenza virus B/Lee/40 (MOI=1) diluted in PBS/BA for 1 h in the dark at RT. After removing the inoculum, cells were incubated either directly with 1 ml DMEM/BA medium containing 2 µg/ml TPCK-treated trypsin (Sigma-Aldrich, USA) at 37°C, 5% CO_2 or Verapamil was added (0.0, 0.1, 1.0, 10, 25, 50, 100, 250, 500 µM) 2 h p.i. to the media. Samples of the supernatants were collected at 24 h p.i., which were then assayed by focus assay for further determination of the amount of infectious virus. The results represent the averages of 3 biological replicates experiments. After removing the inoculum, cells were incubated with 1 ml DMEM/BA medium containing 1 µg/ml TPCK-treated trypsin (Sigma-Aldrich, USA) at 37 °C, 5% CO_2.

To determine the EC_{50}, viral titres of the cell culture supernatants were calculated in percentage. The number of FFU of the untreated virus-infected control was set as 100% and the titres of Verapamil treated samples were calculated as follows: Percentage inhibition =100/(FFU virus-infected sample x Verapamil treated sample). The EC_{50} value (i.e. the concentration of Verapamil required to reduce the virus titre to 50%) was determined using "GraphPad Prism" version 6.00 software for iOS (GraphPad Software, USA) by plotting the percentage virus titre as a function of the Verapamil concentration.

Western blotting

To analyse total viral protein production, PR8-infected A549 cells (MOI=5) were lysed 6 h p.i. and lysates were subjected to Western blot analysis [8]. Briefly, cells were lysed in Triton lysis buffer (TLB: 20 mM Tris–HCl, pH 7.4, 137 mM NaCl, 10% glycerol, 1% Triton X-100, 2 mM EDTA, 50 mM Na-glycerolphosphate, 20 mM Na-pyrophosphate, 5 µg/ml aprotinin, 5 µg/ml leupeptin, 1 mM Na-vanadate, 5 mM

benzamidine) on ice for 30 min by vortexing at 5 min intervals. Cell lysates were then centrifuged at 13 000 xg for 30 min at 4°C and protein concentration was determined by Bradford assay. Cell lysate was subjected to SDS–PAGE and blotted on polyvinylidene fluoride (PVDF) membranes (Millipore Immobilon-P transfer membranes, Roth, Germany). Membranes were incubated with primary rabbit polyclonal anti-PR8 anti-serum (1:500, kindly provided by M. Matrosovich, Marburg, Germany). Proteins recognized by primary antibodies were further incubated with Infrared IRDye-conjugated goat anti-rabbit monoclonal secondary antibody (1:10.000 Li-Cor, Germany).

RNA isolation and primer extension assay

Confluent A549 cells in 35 mm dishes (n=3) were infected with PR8 (MOI=3) and treated with or without Verapamil or U0126 as mentioned above at the indicated concentrations. Total cellular RNA was extracted with Trizol reagent (Invitrogen, Germany) at 8 h p.i. Primer extension was performed as previously described [18] using 1 µl RNA (approximately 3 µg) mixed with an excess of respective DNA primer, labelled at the 5' end with γ32P-ATP (approximately 105 cpm), and denatured by heating at 95°C for 3 min. The mixture was cooled on ice and 100 units of SuperScript III reverse transcriptase (Invitrogen, Germany) and its reaction buffer containing dNTPs (Invitrogen, Germany) were added before further incubation at 50°C for 1 h. The gene-specific DNA primer used for NP vRNA (5'- TGATGGAAAGTGCAAGACCA- 3') results in a product with an expected size of 181 nt, and the gene-specific primer for NP mRNA and cRNA (5'- TGATTTCAGTGGCATTCTGG- 3') results in a product of an expected size of 121 nt for cRNA and 135 nt for mRNA, approximately. A primer for cellular 5S rRNA (5'-TCCCAGGCGGTCTCCCATCC-3') was used as an internal control. Transcription products were analysed on 6% polyacrylamide gels containing 7 M urea in Tris-borate-EDTA (TBE) buffer. The accumulation of RNA species was detected using a phosphoimager (Typhoon 9200, GE Healthcare, USA). For quantification the software package "Quantify One" (Bio-Rad, USA) was applied. The values for vRNA, cRNA and mRNA were normalized to 5s RNA values and were converted to mean percentages of RNA species expression compared to untreated sample (100%), and presented in a graphical format using "GraphPad Prism 5" software package (GraphPad Software Inc., USA). The significance of the data was tested using a two-tailed one-sample t-test.

Chloramphenicol-Acetyltransferase (CAT) assay

To determine the effect of Verapamil on the viral polymerase activity by CAT assay, 293T cells were transfected in triplicates with 2 µg pPol I-CAT-RT [21] using 4 µl of TransIT-2020 (Mirus, USA) and incubated for 8 h. The transfected 293T cells were then infected with PR8 (MOI=3), 1 h at 37°C. The transfected/infected 293T cells were incubated with or without Verapamil (200 µM, added 2 h p.i.) in DMEM/BA for 24 h at 37°C/5% CO_2 before CAT protein expression was analysed. Alternatively, the cells were transfected with the pHMG-CAT plasmid (2 µg) leading to a Pol II-dependent CAT expression and were further incubated in DMEM/BA with or without Verapamil (200 µM) for 24 h at 37°C/5% CO_2 before CAT protein expression was analysed. Briefly, cells were washed with PBS^{++}, scraped-off in 500 µl PBS^{++} and transferred into a new reaction cup (on ice). Cells were then precipitated at 3000 rpm, 4°C for 1 min. The cell pellet was resuspended in 100 µl of 0.25 M Tris-HCl (pH-7.4) and incubated for 2 min in liquid nitrogen followed by 5 min incubation at 37°C in a water bath. This process was repeated for two more times and cell debris was precipitated at 3000 rpm, 4°C for 1 min. 100 µl supernatant was transferred into a new reaction cup on ice and was directly analysed for CAT activity or was stored at -7°C. Next, 50 µl of pre-diluted enzyme extract (10^{-1}, 10^{-2}, 10^{-3}) was mixed with 20 µl Acetyl Co-enzyme A (4 mM, Sigma Aldrich, Germany) and 5 µl BODIPY (Invitrogen, USA) and incubated at 37°C for 2.5 h. Thereafter, 500 µl of ethyl acetate (Roth, Germany) was added and mixed vigorously for 5 min, and then the phases were separated at 13.000 rpm for another 5 min afterwards, 450 µl of the upper ethyl acetate layer was transferred into new reaction cup and dried under vacuum for 30 min. The dried pellet was dissolved with 20 µl ethyl acetate and loaded on a silica gel TLC plate (Merck, Germany). The products were then separated with running buffer (30% methanol, 70% chloroform) in an inclined position. The products (acetylated Chloramphenicol) and the non-acetylated substrate were visualized, scanned and quantified using a Typhoon 9200 (GE Healthcare, USA) and with the "GenQuant" software package (GE Healthcare, USA).

Luciferase reporter assay

The Luciferase reporter gene assay was performed as previously described [22]. Briefly, confluent 293T monolayers in 6-well plates (2×10^6 293T cells/well) were co-transfected with expression plasmids encoding the PB2 (pCAGEN-PB2, 1 µg), PB1 (pCAGEN-PB1, 1 µg), PA (pCAGEN-PA, 1 µg) and NP (pCAGEN-NP, 2 µg) protein of influenza virus B/Ned/537/05 together with the Pol I-dependent luciferase reporter plasmid (pHH-B-vNS-Luc, 2 µg) in a ratio of 1:1:1:2:2 using TransIT-2020 (Mirus, USA) as previously described [23,24]. After transfection, cells were kept with Opti-MEM (Invitrogen, Germany) containing 0.2 % BA and antibiotics. 2 h post transfection, three wells out of the six were treated with Verapamil at a final concentration of 200 µM. After 24 h, the cells were harvested, washed, lysed with 35 µl of "1x passive lysis buffer" (Promega, USA). Next, 100 µl of "1x luciferase substrate solution" (436 µM D-luciferin, 436 µM NaOH, 20 mM Tricin, 2.67 mM $MgSO_4$, 1.07 mM Mg carbonate hydroxide, 33 mM DTT, 530 µM ATP, and 290 µM CoA) were added to 25 µl of cell lysate. The luciferase activity was measured using a microplate luminometer (MicroLumatePlus LB 96V; Berthold Technologies, Germany).

Immunofluorescence and confocal laser scanning microscopy

A549 cells were seeded on 8-chamber culture slides (BD Falcon, USA), infected and incubated as described above. The cells were washed with PBS^{++} at 8 h p.i. and fixed with 4 % PFA (Roth, Germany) in PBS^{++} at RT for 1 h. For permeabilization the cells were incubated in 1 % Triton X-100 in PBS^{++} at RT for 45 min. Then cells were incubated with the primary antibody (mouse α-IVA NP (FPV) mAb, clone 1331, 1:1000, Biodesign, USA) in PBS^{++} containing 3% BSA at RT for 1 h. After washing in PBS^{++}, the Alexa Fluor 594 F(ab´)2 fragment-coupled goat anti-mouse secondary antibody (1:200, Molecular Probes, Germany) was added and incubated in the dark for 1 h. Subsequently the cells were washed again in PBS^{++} and incubated in the dark with DAPI (2.5 µg/ml, Roth, Germany) for 10 min. After the staining, the cells were washed with PBS^{++} and dH_2O and embedded in Mowiol (Sigma-Aldrich, Germany) solved in glycerol and H_2O supplemented with 2.5 % DABCO [1,4-diaza-bicyclo(2.2.2)octane] (Merck, Germany). Fluorescence was visualized with a confocal laser-scanning microscope (Leica TCS SP5, Germany).

Production of Influenza pseudotyped retroviral particles and transduction assays

Influenza H5N1-pseudotyped retroviral particles with the HA, NA and M proteins of the influenza virus strain A/Thailand/KAN-1/2004 (KAN-1, H5N1) carrying the GFP-reporter gene were generated as previously described [17].

To determine the transduction efficiency and the infectious titre, A549 target cells were seeded at a density of 5 x 10^4 cells per well in 24-well plates 24 h before transduction. Serial dilutions of H5N1-pseudotyped retroviral particles were added to the cells and the cultures were incubated for 72 h at 37 °C. The percentage of GFP-positive cells was determined by FACS analysis and the infectious titres were calculated by using the formula: titre = % GFP-positive cells x (5 x 10^4/100) x dilution factor.

Entry-inhibition assay using H5N1 pseudotyped retroviral particles

To determine the inhibitory capacity of Verapamil on entry of the H5N1-pseudotyped virus particles an entry-inhibition assay was performed [17]. Briefly, 1 × 10^4 A549 cells per well were seeded in a 96-well plate and incubated for 24 h (n=2). For each well 4 µl of the H5N1-pseudotyped particle stock (5.13 × 10^5/ml) was diluted in 46 µl medium. The mixture was added to the cells followed by the addition of 50 µl Verapamil dilutions with different concentrations at variable time points (0, 0.5, 1, 1.5, 3, 5, and 24 h). As control 1 µg of a neutralizing mouse anti-HA mAb (CIB 5-25, kindly provided by Dr. R. Tanasa, University Bucharest, Romania) was added under the same conditions. Verapamil and antibody dilutions were prepared in dH_2O. All cultures were incubated at 37°C. 72 h after the transduction with the H5N1-pseudotyped particles the percentage of GFP-positive cells was determined by FACS-analysis. The received values were normalized to the virus-only control using "GraphPad Prism 5" software package (GraphPad Software Inc., USA).

NF-κB activity analysis

Detection of active NF-κB was performed with an ELISA based high-throughput screening system (TransAM, ActiveMotif, USA) according to the manufacturer´s instruction [10]. Briefly, in this assay, immobilized oligonucleotides containing an NF-kB (5′-GGACTTTCC-3′) consensus binding sequence detect only the active form of NF-κB that will bind to this site. NF-κB dimers can only bind DNA after activation and translocation into the nucleus; therefore, only NF-κB dimers present in the nucleus are measured in the DNA/protein binding assay and inactive cytosolic NF-κB will not be measured. The primary antibodies used then to detect bound NF-κB recognize an epitope on p65 that will only be accessible when NF-κB is active and bound to the target DNA. A secondary HRP-conjugated antibody is used for colorimetric analysis via spectrophotometry.

In our study, PR8-infected (MOI=5) A549 cells (n=3), treated as mentioned before, were lysed in TLB at the indicated time points p.i. and collected for further analysis. The assay was performed according to the manufacturer's protocol and analysed by ELISA reader (Biotek EL808, USA) at 450 nm wavelength.

IkBα activation

Detection of phospho-IkB-α was performed by Western blot (n = 2). Briefly, PR8-infected (MOI=5) A549 cells were treated with or without 200 µM Verapamil in infection media 2 h p.i. At the indicated time points p.i. cells were lysed in TLB. Cell lysate was cleared by centrifugation, and protein concentration was determined by Bradford assay before subjection to SDS–PAGE and blotting onto PVDF membranes. The blots of whole cell lysates were incubated with primary mouse anti phospho-IkBα (Ser32/36) antibody and a primary rabbit anti IkB**α** antibody (1:1.000, Cell Signaling). Membranes were further incubated with Infrared IRDye-conjugated goat anti-mouse and goat anti-rabbit monoclonal secondary antibodies (1:10.000 Li-Cor, Germany) and analysed with an Odyssey detector (Li-Cor, Germany). Quantification of specific bands was done with the Odyssey software package (Li-Cor, Germany). As a positive control uninfected A549 cells were left untreated or were treated with TNFα (10 ng/ml, R&D Systems, USA) for 10 min. Cells were then lysed in TLB to detect IkBα activation as described above. The value for the relative amount of P-IkBα of the TNFα-treated control was set to 100 %.

Viral resistance assay

To investigate the potential emergence of resistant virus variants we performed an resistance assay [25]. Briefly, MDCK-II cells seeded on 24-well plates were infected with PR8 (MOI=0.1). The cells were treated with or without 100 µM Verapamil (2 h p.i.) or 10 µM carboxylic Oseltamivir (directly p.i., Toronto Research Chemicals Inc., CA) and incubated at 37°C, 5% CO_2 for 30 h (n=2, each). The supernatants were collected and samples of either the untreated, Verapamil- or Oseltamivir-treated group were pooled and titrated by focus forming assay to quantify the amount of infectious virus produced. These pooled and titrated supernatants were then used to infect another set of cultures under the same conditions as described above to yield in total 5 rounds of infection and replication. Experiments were stopped when the Oseltamivir sample reached titres of the untreated control.

Results

Verapamil efficiently reduces influenza A and B virus (IAV and IBV) titres in cell culture at non-toxic concentrations

Verapamil (Suppl. Figure 1A) is long known to reduce influenza virus replication [14]. In order to analyse this antiviral effect in more detail, we first defined the cytotoxic concentration of Verapamil at which 50% of A549 cells (as an example for human alveolar epithelia cells) are still viable (CC_{50}). For this, cells were incubated for 24 h with 10 different Verapamil concentrations and cell viability was analysed via MTT assay. We could thereby determine the CC_{50} to be 309.8 µM (Figure 1A).

Next, we analysed the effective concentration of Verapamil at which the virus titre is reduced by 50 % (EC_{50}). For this, A549 cells were infected with influenza virus A/Puerto Rico/8/34 (H1N1) (PR8, prototype example of a human IAV) or influenza virus B/Lee/40 (B/Lee) and treated with Verapamil added 2 h post infection (p.i.) at the indicated concentrations. This delayed addition of Verapamil was done to exclude any effects of Verapamil on early, Calcium-dependent events possibly needed for IAV or IBV replication [12,20]. Virus titres were then analysed after one replication cycle (12 h) and the EC_{50} was calculated to be 7.01 µM for PR8 (Figure 1B) and 14.52 µM for B/Lee virus (Figure 6A). Finally, we determined the antiviral effect of Verapamil on PR8 replication in comparison to the MEK inhibitor U0126 (Figure 1C), which is known to efficiently reduce replication of IAVs and IBVs [8,9]. The results indicate that Verapamil significantly impairs PR8 replication on A549 cells at 100 and 200 µM by up to 90%, which is comparable to U0126.

Verapamil does not influence virus entry

To elucidate whether Verapamil would indeed only be important for late steps in IAV replication as supposed before [14], we performed an entry assay using pseudotyped retroviral particles (PRP) expressing the HA, NA and M2 protein of the influenza virus strain A/Thailand/KAN-1/2004 (KAN-1, H5N1) and carrying the GFP-reporter gene (H5N1-PRP). To determine the entry-inhibition capacity of Verapamil, A549 cells were incubated with a dilution of the H5N1-PRP stock followed by the addition of Verapamil in different concentrations at the indicated time points (0, 0.5, 1, 1.5, 3, 5, and 24 h). As control the neutralizing

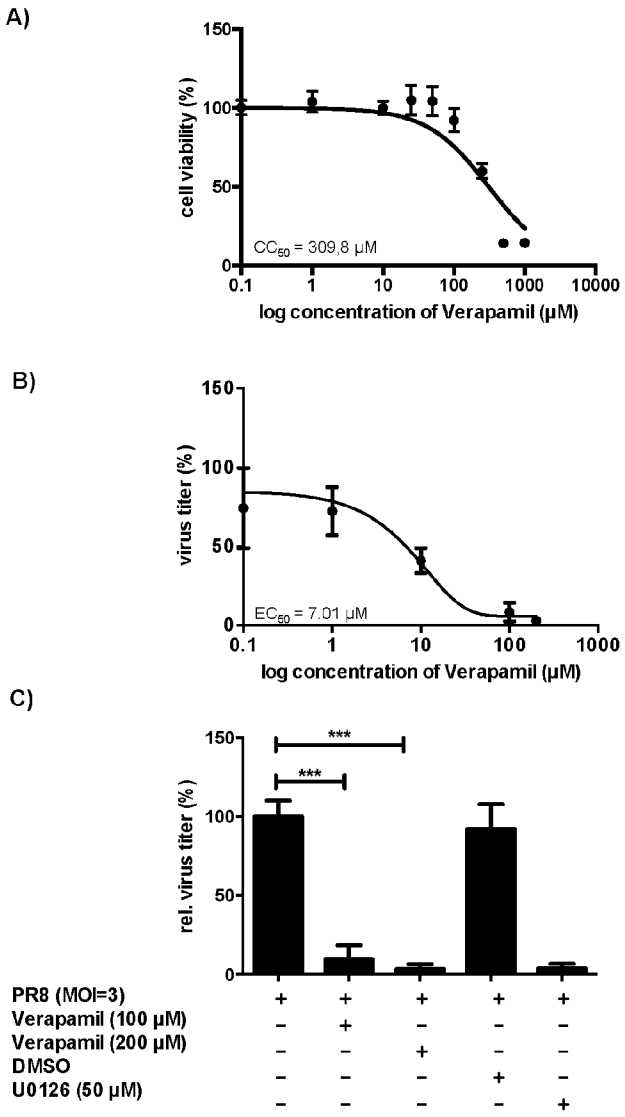

Figure 1: Effects of Verapamil on IAV replication.

To study possible effects of Verapamil on IAV replication, CC_{50} values and EC_{50} values (the latter determined from PR8 titres in the cell culture supernatant) were calculated. **A)** CC_{50} values for A549 cells were determined after treatment with Verapamil for 24 h (n=8). **B)** To determine EC_{50} values, A549 cells (n=3) were infected with PR8 (MOI=1) and treated with the indicated concentrations of Verapamil between 2 and 24 h p.i. Virus titres in cell culture supernatants collected at 24 h p.i. were determined by virus plaque assay. **C)** A549 cells were infected with PR8 (MOI=3) and treated with Verapamil from 2 to 14 h p.i. using the indicated concentrations. As controls, infection experiments were performed in the absence of Verapamil, in the presence of 0.5% DMSO, and U0126 (50 µM), respectively. At 14 h p.i., cell culture supernatants were collected and virus titres determined by plaque assay. Bars reflect ± SEM and were determined from three biological replicates.

mouse anti-HA mAb (CIB5-25) was added under the same conditions. All cultures were incubated at 37°C. 72 h after the transduction with the H5N1-PRPs, the percentage of GFP-positive cells was determined by FACS-analysis. The obtained values were normalized to the virus-only control. The results depicted in Figure 2A show that under Verapamil treatment at no time point post PRP-incubation the percentage of GFP expressing cells is reduced compared to the untreated control. In contrast, the HA-specific mAb effectively reduces the amount of GFP expressing cells up to 4 h post PRP-incubation. Furthermore, A549 cells were either (i) pre-treated with Verapamil (200 µM) 2 h before infection (with PR8, MOI=5) only, (ii) treated 2 h before infection and treated p.i. (starting at 2 h p.i.), (iii) treated post infection only or (iv) were not treated with Verapamil. Virus titres were then determined 12 h p.i.. From the results shown in Figure 2B it is evident that sole pre-treatment of the cells with Verapamil before infection did not impair virus replication, whereas treatment starting 2 h p.i. clearly reduced the virus titre. In conclusion, Verapamil neither affects the entry of PRP, nor does pre-treatment of the cells affect PR8 propagation, indicating that entry of PR8 is not impaired by Verapamil.

Verapamil reduces IAV nuclear RNP export and viral ERK activation in cell culture

In order to elucidate which molecular factors / mechanisms in IAV

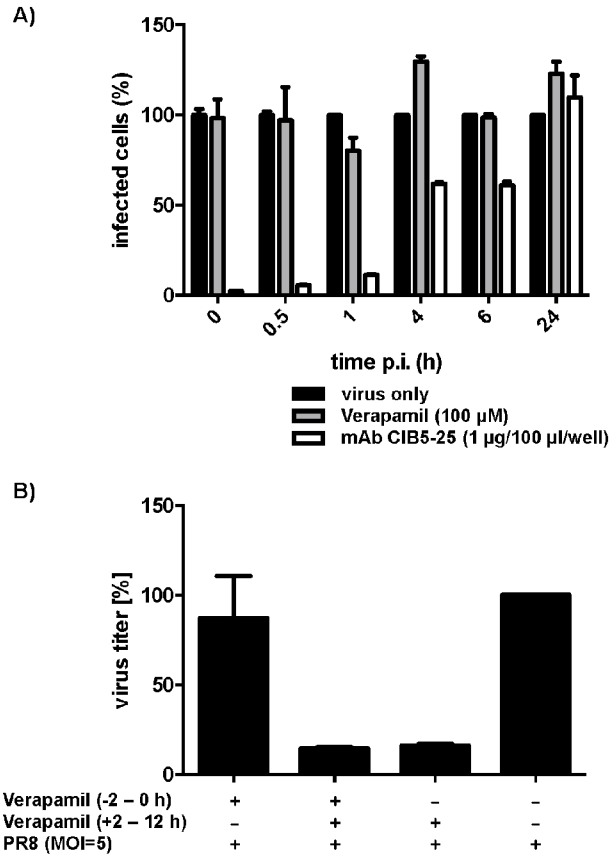

Figure 2: Characterization of possible effects of Verapamil on IAV entry.

To assess possible effects of Verapamil on IAV entry, two approaches were taken. **A)** A549 cells were incubated with H5N1-pseudotyped retroviral particles (PRP) in medium containing 100 µM Verapamil. GFP expression in transduced cells was monitored over time (n=2). As controls, cells were incubated with PRP in the presence of an IAV HA-specific mouse monoclonal mAb (CIB5-25) or without additional treatment. Proportions of GFP-expressing cells were determined by FACS analysis and normalized to the PRP-only control using GraphPad Prism software. **B)** A549 cells were infected with IAV PR8 and treated with 200 µM Verapamil for the following periods of time: (i) for 2 h prior to infection, (ii) from 2 h prior to infection until 12 h post infection, and (iii) from immediately prior to infection until 12 h post infection. As a control, cells were infected with PR8 in kept in medium without Verapamil. Cell culture supernatants were collected at 12 h p.i. and virus titres were determined by plaque assay. Error bars indicate ± SEM as determined from three biological replicates.

replication are affected by Verapamil, we set out to analyse the effect of the substance on a late step in virus replication. We had previously shown that Verapamil inhibits PKCα-dependent ERK activation [12], and that virus-induced ERK activity is an essential pre-requisite for efficient nuclear ribonucleoprotein complexes (RNP) export [8]. Here we attempted to investigate whether Verapamil also alters nuclear RNP export. To this point A549 cells were infected with PR8 and treated either with Verapamil or with the MEK inhibitor U0126. At 8 h p.i. we analysed intra-cellular RNP localization via immunofluorescence using an antibody specific for the viral nucleoprotein (NP), which is the main component of viral RNPs [26], (Figure 3) and found that the RNPs were retained in Verapamil- as well as in U0126-treated cells. Taken together, the results show that Verapamil indeed negatively affects, nuclear RNP export, which represents a plausible cause for the reduced titre observed.

Verapamil impairs the replication and transcription activity of the viral polymerase

Due to the fact that Verapamil affects the nuclear RNP export, we further speculated that the activity of the viral RNA-dependent RNA polymerase (RdRp), which is an integral RNP component, might be affected by Verapamil. The segmented negative strand RNA genome (vRNA) of IAV is replicated via a homologue copy (cRNA) that is synthesized from the vRNA by the viral RdRp, which also generates the viral mRNA directly from the vRNA (reviewed in [27]). We therefore aimed to determine the replicative and transcriptional RdRp activity by analysing the amount of vRNA, cRNA and mRNA produced in infected and Verapamil-treated cells. Confluent A549 cells were infected with PR8 (MOI=3) and treated with or without Verapamil or U0126 at the indicated concentration. Then total cellular RNA was extracted at 8 h p.i. and primer extension was performed as previously described [18]. Verapamil significantly reduced the amount of all three viral RNA species (Figure 4A). The amounts of these three different viral RNA species were quantified and the result gave evidence that Verapamil significantly reduced the amount of the viral RNAs in a concentration-dependent manner (Figures 4B-4D). In contrast, U0126, which also strongly impaired nuclear RNP export (Figure 3A) had no significant effect on the vRNA / mRNA production and only mildly affected

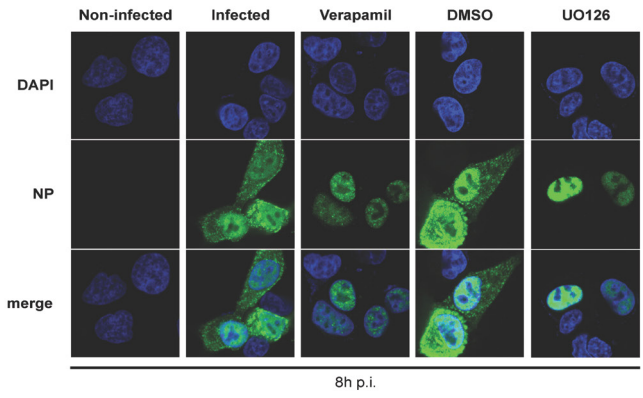

Figure 3: Intra-cellular RNP localization.

To determine possible effects of Verapamil on intra-cellular RNP localization, A549 cells were infected with PR8 (MOI=1). The medium was either supplemented with 200 μM Verapamil (added at 2 h p.i.) or 50 μM UO126 (added directly p.i.). Intra-cellular RNP localization was analysed 8 h p.i. by confocal laser-scanning microscopy using an NP-specific mAb (green). Nuclei were stained with DAPI (blue).

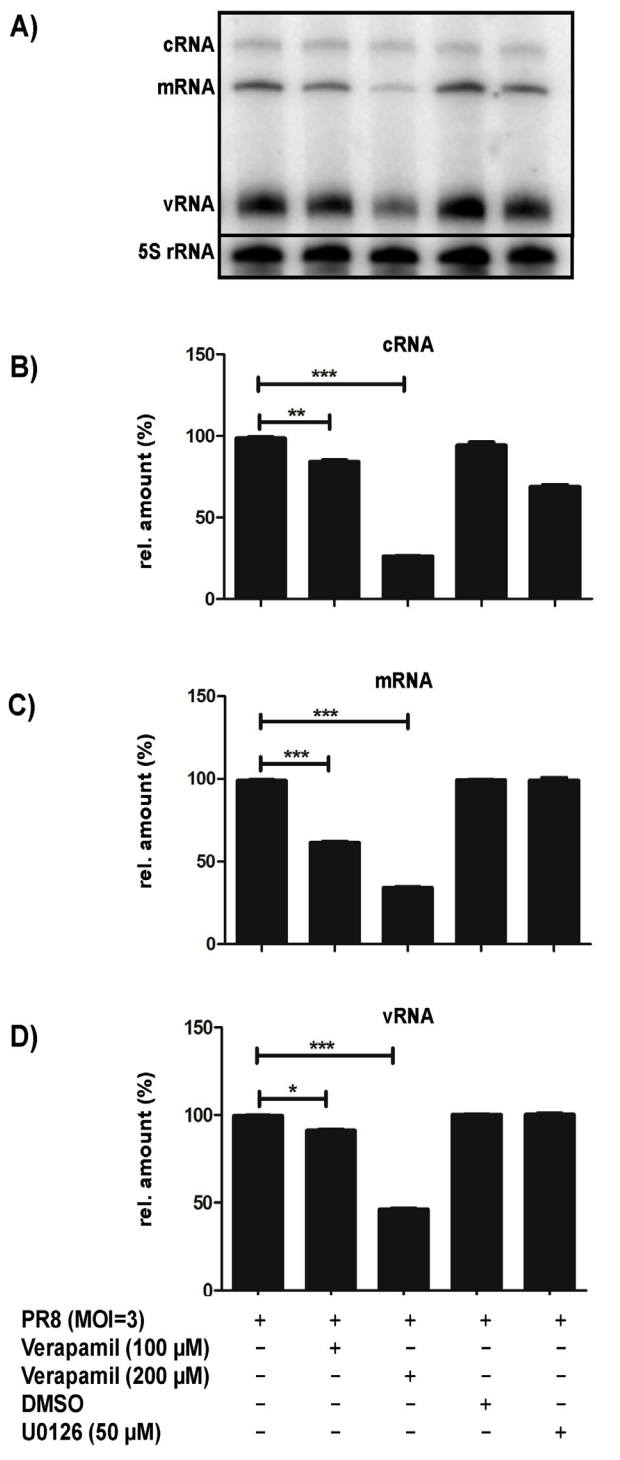

Figure 4: Verapamil affects viral RNA accumulation in infected cells.

A) Primer extension analyses were used to assess possible effects of Verapamil on viral RNA accumulation (synthesis and/or stability). vRNA, mRNA, and cRNA levels at 8 h p.i. in PR8-infected A549 cells (MOI=3) were determined using NP-specific probes (for details, see Material and Methods). Cells were either untreated or treated from 2 to 8 h p.i. with Verapamil or controls (0.5% DMSO; 50 μM U0126) as indicated. 5S rRNA served as a loading control. **B-D)** Quantification of the vRNA, mRNA and cRNA accumulation data (using 5S rRNA for normalization). Error bars indicate ±SEM as determined from three independent experiments (one of which is shown in **A**).

cRNA amounts, supporting earlier findings [8]. These results indicate that Verapamil impairs PR8 propagation by decreasing RdRp activity leading to reduced genome amplification and viral mRNA production resulting in reduced formation of new infectious progeny virions.

Verapamil decreases viral protein production

Preceding results showed that viral mRNA was diminished by Verapamil. Therefore, we further extended our investigation to analyse the effect of Verapamil on the generation of viral proteins (Figure 5). To achieve this, A549 cells were infected with PR8 at the indicated MOI and were treated with Verapamil (100, 200 µM) or with U0126 (50 µM) as control. Verapamil treatment led to an obvious reduction in the amount of viral proteins that were detected with a PR8 specific serum (Figure 5A). In contrast, U0126 did not affect RdRp activity nor did it reduce the amount of viral proteins.

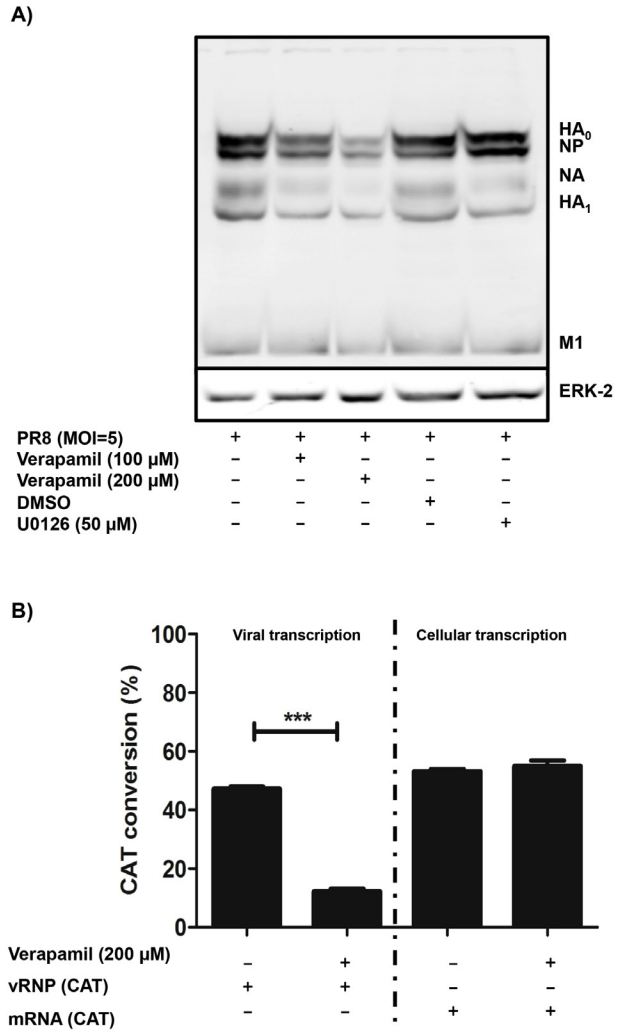

Figure 5: Verapamil reduces viral protein production.

A) Western blot analysis of cell lysates obtained from PR8-infected A549 cells at 8 h p.i. using a PR8-specific antiserum. ERK-2 was detected as a loading control. Infections were done in the absence/presence of Verapamil and controls, respectively, as indicated below the blot. **B)** A CAT reporter assay was used to study possible effects of Verapamil on IAV RdRp activity. 293T cells were transfected with a plasmid expressing a vRNA-like Pol-I transcript encoding the CAT gene (viral transcription) and subsequently infected with PR8. Alternatively, cells were transfected with a plasmid that allowed Pol-II-dependent expression of the CAT gene (cellular transcription). Verapamil was included or not included as indicated. CAT activity was determined at 12 h p.i. and 8 h post transfection, respectively. Error bars represent ±SEM as determined from of three independent experiments.

Furthermore, we investigated the specificity of the Verapamil effect on the activity of the viral RdRp by transfecting A549 cells with a plasmid for the *in vitro* generation of a vRNA-like Pol1-transcript encoding the chloramphenicol-acetyl transferase (CAT) protein as a reporter for the replication/transcription activity of the RdRp [21]. These cells were then infected with PR8 providing the RdRp activity *in trans* and CAT activity with or without Verapamil treatment was determined (Figure 5B). Also here, we detected a significant reduction of CAT activity of the transfected cells that were treated with Verapamil. As a control we had transfected cells with a plasmid for Pol2-dependent CAT expression, representing cellular transcription/translation activity and could not detect any reduction in CAT activity.

To assay the impact of Verapamil on RdRp activity of IBV, a luciferase reporter assay was used. A plasmid expressing a vRNA-like Pol1-transcript encoding the luciferase gene was co-transfected into 293T cells together with plasmids expressing the RNP-constituting proteins of B/Ned/537/05 (PB1, PB2, PA, NP) in the presence and absence (control) of Verapamil. Notably, Verapamil treatment led to a significant decrease in the luciferase activity (corresponding to RNP activity of B/Ned/537/05) (Figures 6A and 6B). These results suggest that Verapamil specifically impairs the activity of the viral RdRp of IAV and IBV, but not the cellular transcription/translation. Furthermore, they indicate that no other viral proteins are needed to exert the effect of Verapamil treatment.

Virus-induced NF-kB activation is reduced by Verapamil treatment

The central step in the canonical NF-κB pathway is the activation of

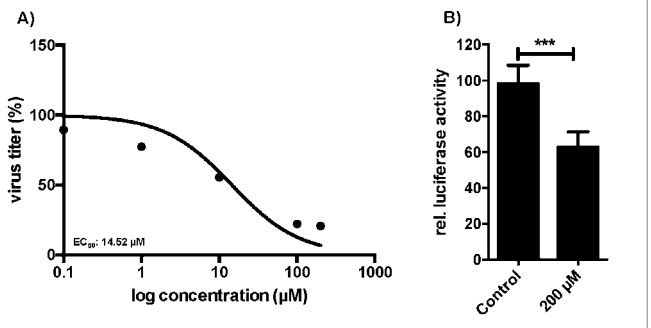

Figure 6: Effect of Verapamil on influenza B virus replication

Virus titres in culture supernatants obtained from B/Lee-infected cells and viral polymerase activities determined by CAT reporter assays, respectively, were used as markers for studying IBV replication in the presence or absence of Verapamil. **A)** A549 cells (n=3) were infected with B/Lee (MOI=1) and Verapamil was added at 2 h p.i. using the indicated concentrations. For comparison, infected A549 cells were treated directly p.i. with solvent control (H_2O). At 14 h p.i., cell culture supernatants were collected and virus titres determined by plaque assay. **B)** To investigate possible effects of Verapamil on the viral RdRp activity of an influenza B virus, 293T cells were co-transfected (using a molar ratio of 1:1:1:2:2) with pCAGEN expression plasmids encoding the PB2, PB1, PA and NP proteins of the influenza B/Ned/537/05 virus, along with pHH-B-vNS-Luc plasmid DNA, the latter containing a luciferase reporter gene under control of a Pol I-promoter (n=3). At 2 h post transfection, cells were treated with Verapamil in a final concentration of 200 µM or left untreated (control). At 24 h p.i., the cells were lysed and luciferase activities determined. Error bars reflect ± SEM as determined from three independent experiments.

the IκB kinase (IKK) complex, which is composed of the kinases IKKα and IKKβ and the scaffold protein NEMO (NF-κB essential modulator). The activated IKK complex phosphorylates the inhibitory IκB (inhibitor of NF-κB), leading to its subsequent proteolytic degradation, which allows the DNA binding subunits of NF-κB to enter the nucleus and to bind to their target DNA to activate transcription [28].

Previously we demonstrated that IAV caused the NF-κB-dependent induction of Tumour Necrosis Factor-related Apoptosis-inducing Ligand (TRAIL) and Fas/FasL, which is crucial for efficient IAV propagation [15]. As Verapamil impairs phorbol 12-myristate 13-acetate (PMA)-induced activation of NF-κB [29] we asked whether Verapamil might also influence the IAV-induced NF-κB activation. To this end, A549 cells were infected with PR8 (MOI=5) and analysed for the activation of NF-κB by determining the amount of activated/phosphorylated IkB (P-IκB-α) at the indicated time points p.i. (Figure 7A). The results show that at all times the amount of P-IκB-α is reduced in PR8-infected and Verapamil-treated cells. Consequently, we further analysed the amount of active NF-κB in PR8-infected and Verapamil-treated cells at the indicated time points p.i. (Figure 7B). According to the results concerning the amount of activated IκB-α, Verapamil treatment obviously reduced the amount of PR8-induced active NF-κB. Therefore, it is tempting to speculate that this further adds to the antiviral activity of Verapamil against IAV.

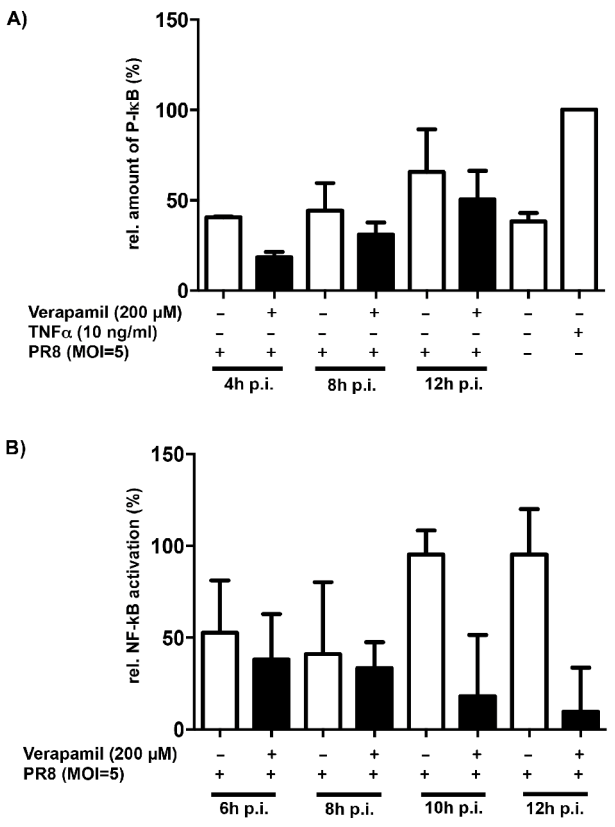

Figure 7. Effect of Verapamil on virus-induced NF-κB activation

A) To analyse possible effects of Verapamil treatment on NF-κB activation, the amount of phospho-IκB-α in lysates obtained from PR8-infected A549 cells (MOI=5) that were treated with 200 µM Verapamil (black bars) or left untreated (white bars) was determined by Western blotting at the indicated time points p.i.. The blots were incubated with mouse anti-phospho IκB-α and rabbit anti-ERK2 antibody (loading control). Specific immune complexes were detected using suitable secondary antibodies and the LI-COR Odyssey imaging system including software. As a control, uninfected cells were treated with TNFα (positive control) or left untreated. The value obtained for the TNFα-treated control was set to 100%. Error bars reflect ± SEM as determined from three independent experiments.

B) Quantification of active NF-κB was done using an ELISA-based assay in which immobilized oligonucleotides containing an NF-κB consensus-binding sequence are used to specifically bind/detect the active form of NF-κB. PR8-infected A549 cells (MOI=5), treated with 200 µM Verapamil (black bars) or untreated (white bars), were collected at the indicated time points p.i. and active NF-κB was determined in lysates obtained from these cells. Error bars reflect ± SEM as determined from three independent experiments.

Verapamil does not induce the emergence of resistant PR8 variants

The direct targeting of IAV replication via antibodies or chemical compounds generally leads to viral resistance due to the high genetic plasticity of the virus [5]. Therefore, it is of great importance to elucidate whether treatment with an antiviral substance leads to the emergence of resistant IAV variants. As we have shown that Verapamil does affect the RdRp activity, we asked whether this would lead to viral resistance against Verapamil. Along this line, we infected MDCK-II cells with PR8 at a low MOI=0.1 to allow multi-cycle replication. We chose MDCK-II cells, because they support higher replication of PR8 than A549 cells and consequently should also generate higher numbers of genetic variants. The cells were then treated with or without 100 µM Verapamil (2 h p.i.) or 10 µM Oseltamivir (directly p.i.) as a positive control for the generation of resistant variants. After 30 h the supernatants of each group (untreated, Verapamil or Oseltamivir treated) were collected and titred to quantify the amount of infectious virus produced. These supernatants were used for a next round of infection under the same conditions as described above to yield in total 5 rounds of infection and replication. Experiments were stopped, when the Oseltamivir sample reached titres of the untreated control (100%). In contrast to the Oseltamivir treatment, which was highly effective in the first round, but lost its effectiveness after a total of 5 rounds, Verapamil does not induce the emergence of resistant PR8 variants within 5 passages (Figure 8) indicating that Verapamil might not lose its antiviral capacity over time.

Discussion

Influenza virus (IV) is considered to be a common and serious human pathogen that annually leads to significantly high morbidity and mortality worldwide. Besides vaccination, neuraminidase inhibitors (NAI) are currently the available treatment of choice against influenza. However, NAI-resistant IV have already been reported due to continuous high rate of mutation [30,31]. Therefore, there is still an urgent necessity to look for new antiviral drugs with novel modes of action to overcome IV infection. In this regard the present study investigated the related modes of antiviral activity of Verapamil.

Verapamil was previously reported to affect cytomegalovirus replication [32], mouse mammary tumour virus expression [33], human rhinovirus 2 release [34], budding of Sindbis- and vesicular stomatitis viruses [35] as well as measles- and vaccinia virus replication [36].

Herein, we show that Verapamil efficiently impairs PR8 replication on A549 cells does-dependent at sub-toxic concentrations by up to 90%, which is comparable to the MEK inhibitor U0126. More recently, Verapamil was reported to inhibit infection with the Junin virus and with filoviruses (e.g. Ebola and Marburg viruses) by blocking their entry [37,38]. However, we found that Verapamil does not influence the entry of pseudotyped retroviral particles (PRP) expressing the HA,

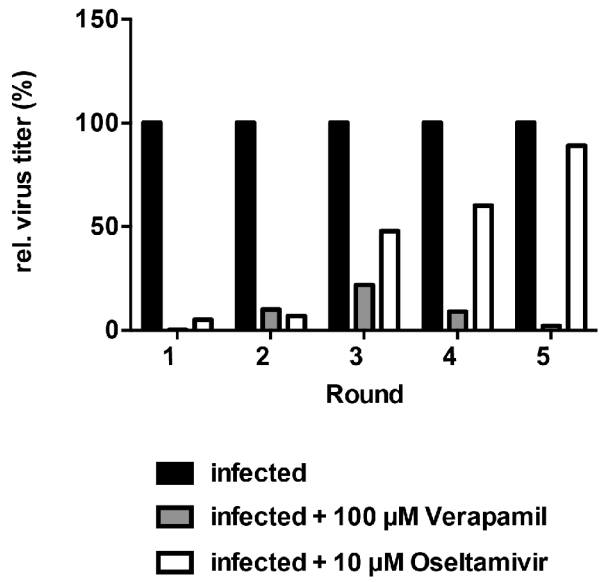

Figure 8: No evidence for Verapamil-resistant variants emerging upon serial passaging of IAV PR8.

To assess the potential for the emergence of viral variants with reduced sensitivity to Verapamil treatment, MDCK-II cells were infected with PR8 (MOI = 0.1) and the culture medium was supplemented with Verapamil (added at 2 h p.i.) and Oseltamivir (added directly p.i.), respectively. Infected cells (without drug) were used as a control. At 30 h p.i., supernatants (n=2) of the untreated, Verapamil- and Oseltamivir-treated group, respectively, were pooled and virus titres were determined by focus-forming assay. Virus-containing supernatants of each of the groups were subjected to another 5 rounds of infection using the same conditions (MOI=0.1). Relative numbers of infectious virus particles obtained at each passage from cultures treated with 100 µM Verapamil and 10 µM Oseltamivir, respectively, are given. Values (in percentage) are given in relation to the virus titres obtained from infected cells without treatment (which were set to 100 %).

NA and M1 protein of the influenza A/Thailand/KAN-1/2004 (KAN-1, H5N1) carrying the GFP-reporter gene into mammalian A549 cells. Furthermore, pre-treatment of the cells with Verapamil before PR8-infection alone also did not affect virus replication, whereas Verapamil treatment starting 2 h post infection strongly reduced the virus titer. These results indicate that the inhibitory effect of Verapamil against PR8 does not involve viral entry.

Beside its calcium channel blocking activity, Verapamil also affects PKC activation [14]. In IV-infected cells, the PKC inhibition impairs ERK-activation [12], which is essential for efficient nuclear RNP export at the late stage (6-10 h p.i.) of the viral life cycle and therefore for virus production [8]. In our present investigation of the anti-IV mode of action, we found that Verapamil impedes nuclear RNP export in a dose dependent manner in cell culture. Therefore, it is tempting to speculate that Verapamil could impair the formation of new infectious progeny by hindering nucleo/cytoplasmic RNP transport. Furthermore, we hypothesized that not only RNP-transport, but also the RdRp activity might be affected. This was indeed the case, as Verapamil treatment significantly reduced the production of all three viral RNA species (vRNA, cRNA, mRNA) in a dose-dependent manner (Figure 4). Importantly, the MEK inhibitor U0126, which also strongly impaired nuclear RNP export (Figure 3) did not show a notable impact on the RdRp activity (Figure 4). Furthermore, Verapamil significantly reduced CAT expression of a vRNA-like Pol-I transcript encoding the CAT gene (reporter vRNA) in subsequently PR8-infected cells, which in contrast was not affected by U0126 (Figure 4B). Similarly, the overall production of viral proteins in PR8-infected and Verapamil-treated cells was decreased (Figure 5A). Based on these results, it can be hypnotized that Verapamil treatment either directly or indirectly (via specific cellular or viral proteins) causes a specific impairment of the viral RdRp replication and transcription activity (mRNA synthesis) and consequently the reduction of viral protein production.

Previously, it was shown that NF-κB-dependent induction of the pro-apoptotic factors TRAIL and Fas/FasL is crucial for efficient IAV propagation and that different NF-κB inhibitors are able to reduce IV propagation [10,15,25]. Additionally, it was demonstrated that activation of the apoptotic Caspase 3 is also important for efficient IV propagation [39] as IV-induced Caspase-dependent enlargement of nuclear pores promotes nuclear export of the viral RNPs [16]. Current understanding therefore proposes a model that connects the observed events, e.g. virus-induced NF-κB activation, Caspase induction and nuclear RNP export. During productive virus infection the pro-apoptotic factors TRAIL, Fas and FasL are expressed in an NF-κB-dependent manner. These factors induce Caspase activation in an auto- and paracrine fashion via the extrinsic apoptosis pathway. Active Caspases then allow an enhanced release of RNP complexes from the nucleus, due to Caspase-mediated disruption of the active nuclear pore complex (for review see [40]). As it was shown that Verapamil impairs phorbol 12-myristate 13-acetate (PMA)-induced activation of NF-κB [29] we analysed whether Verapamil might also influence the IV-induced NF-κB activation. The results obtained revealed that IAV-induced NF-κB activation is indeed impaired by Verapamil treatment, which might contribute to a negative effect on IV replication.

In recent years, the evolution of viral drug resistance is a major drawback for the currently prescribed anti-influenza neuraminidase inhibitors (NAI) [30,31]. Unlike Oseltamivir, which is designed to inhibit the activity of the (mutable) viral neuraminidase, we found that Verapamil, which in addition targets cellular factors implicated in IV replication, does not induce the emergence of resistant PR8 variants in five rounds of replication.

The fact that all the observed antiviral effects of Verapamil should collectively contribute to the total impact of Verapamil on the production of progeny virions, could explain why the Verapamil concentration needed to reduce the number of infectious virus particles by 50% is lower than the concentration needed to clearly observe an effect in a particular assay used to analyse a specific mechanism/factor. This discrepancy between the EC_{50} and the concentration needed to observe the paricular effects requests further investigations of additional activities/effects of Verapamil besides its Ca-channel inhibition. Verapamil is an approved drug used in treatment of hypertension, angina pectoris and cardiac arrhythmia, therefore it needs to be analysed whether it has an anti-IV potential without causing cardio-vascular effects.

Taken together, we investigated in more detail the effect of Verapamil on influenza virus propagation and could identify mechanisms/factors implied in the antiviral effect of Verapamil, which to the best of our knowledge has not been done before. We show that Verapamil exerts several negative effects on IV propagation and might prevent evolution of viral resistance.

Acknowledgements

We thank S. Ludwig, Munster, Germany, for providing the mouse anti-Influenza A virus nucleoprotein mAb, R. Tanasa, Bucharest, Romania, for providing the mouse anti-HA mAb (CIB 5-25), and M. Matrosovich, Marburg, Germany, for providing the rabbit anti-PR8 serum. Furthermore, we would like to thank L. Naesens, Leuven, Belgium, for providing the expression plasmids PB2, PB1, PA

and NP of influenza virus B/Ned/537/05 and pHH-B-vNS-Luc, which we used in a mini-replicon assay for influenza B virus. We also thank K. Nagata, Tsukuba, Japan, for the firefly luciferase reporter plasmid pHH-B-vNS-Luc. We are grateful to E. Erdogan and M. Riedl for their excellent technical assistance. This work was supported by the DFG-funded International Research Training Group "Enzymes and Multienzyme Complexes Acting on Nucleic Acids" (IRTG 1384 graduate scholarship to M.I.A.) and in part by the German Centre for Infection Research (DZIF), partner site Giessen, funded by the German Federal Ministry of Education and Research (BMBF, to S.P and J.Z.), the DFG-funded Transregional Collaborative Research Centre "Innate Immunity of the Lung: Mechanisms of Pathogen Attack and Host Defence in Pneumonia" (SFB/TR 84, to S.P.), the DFG-funded Collaborative Research Centre 1021 "RNA viruses: RNA metabolism, host response and pathogenesis" (SFB1021; projects A01 and C01 to J.Z. and S.P., respectively) and by a fellowship of the German-Egyptian Research Long-Term Scholarship "GERLS" program co-funded by the Egyptian government and the German Academic Exchange Service (DAAD, to A.M.). The funders had no role in study design, data collection and analysis, decision to publish, or preparation of the manuscript.

References

1. Meng Z, Han R, Hu Y, Yuan Z, Jiang S, et al. (2014) Possible pandemic threat from new reassortment of influenza A(H7N9) virus in China. Euro Surveill 19.
2. Richard M, de Graaf M, Herfst S (2014) Avian influenza A viruses: from zoonosis to pandemic. Future Virol 9: 513-524.
3. Houser KV, Katz JM, Tumpey TM (2013) Seasonal trivalent inactivated influenza vaccine does not protect against newly emerging variants of influenza A (H3N2v) virus in ferrets. J Virol 87: 1261-1263.
4. Moscona A (2009) Global transmission of oseltamivir-resistant influenza. N Engl J Med 360: 953-956.
5. Ludwig S, Planz O, Pleschka S, Wolf T (2003) Influenza-virus-induced signaling cascades: targets for antiviral therapy? Trends Mol Med 9: 46-52.
6. Planz O (2013) Development of cellular signaling pathway inhibitors as new antivirals against influenza. Antiviral Res 98: 457-468.
7. Pleschka S (2008) RNA viruses and the mitogenic Raf/MEK/ERK signal transduction cascade. Biol Chem 389: 1273-1282.
8. Pleschka S, Wolff T, Ehrhardt C, Hobom G, Planz O, et al. (2001) Influenza virus propagation is impaired by inhibition of the Raf/MEK/ERK signalling cascade. Nat Cell Biol 3: 301-305.
9. Ludwig S, Wolff T, Ehrhardt C, Wurzer WJ, Reinhardt J, et al. (2004) MEK inhibition impairs influenza B virus propagation without emergence of resistant variants. FEBS Lett 561: 37-43.
10. Pinto R, Herold S, Cakarova L, Hoegner K, Lohmeyer J, et al. (2011) Inhibition of influenza virus-induced NF-kappaB and Raf/MEK/ERK activation can reduce both virus titers and cytokine expression simultaneously in vitro and in vivo. Antiviral Res 92: 45-56.
11. Droebner K, Pleschka S, Ludwig S, Planz O (2011) Antiviral activity of the MEK-inhibitor U0126 against pandemic H1N1v and highly pathogenic avian influenza virus in vitro and in vivo. Antiviral Res 92: 195-203.
12. Marjuki H, Alam MI, Ehrhardt C, Wagner R, Planz O, et al. (2006) Membrane accumulation of influenza A virus hemagglutinin triggers nuclear export of the viral genome via protein kinase Calpha-mediated activation of ERK signaling. J Biol Chem 281: 16707-16715.
13. Lullmann H, Mohr K, Hein L (2006) Pharmakologie und Toxikologie 16. Thieme.
14. Nugent KM, Shanley JD (1984) Verapamil inhibits influenza A virus replication. Arch Virol 81: 163-170.
15. Wurzer WJ, Ehrhardt C, Pleschka S, Berberich-Siebelt F, Wolff T, et al. (2004) NF-kappaB-dependent induction of tumor necrosis factor-related apoptosis-inducing ligand (TRAIL) and Fas/FasL is crucial for efficient influenza virus propagation. J Biol Chem 279: 30931-30937.
16. Muhlbauer D, Dzieciolowski J, Hardt M, Hocke A, Schierhorn KL, et al. (2015) Influenza Virus-Induced Caspase-Dependent Enlargement of Nuclear Pores Promotes Nuclear Export of Viral Ribonucleoprotein Complexes. J Virol 89: 6009-6021.
17. Schmier S, Mostafa A, Haarmann T, Bannert N, Ziebuhr J, et al. (2015) In Silico Prediction and Experimental Confirmation of HA Residues Conferring Enhanced Human Receptor Specificity of H5N1 Influenza A Viruses. Sci Rep 5: 11434.
18. Wang Z, Robb NC, Lenz E, Wolff T, Fodor E, et al. (2010) NS reassortment of an H7-type highly pathogenic avian influenza virus affects its propagation by altering the regulation of viral RNA production and antiviral host response. J Virol 84: 11323-11335.
19. Root CN, Wills EG, McNair LL, Whittaker GR (2000) Entry of influenza viruses into cells is inhibited by a highly specific protein kinase C inhibitor. J Gen Virol 81: 2697-2705.
20. Sieczkarski SB, Brown HA, Whittaker GR (2003) Role of protein kinase C betaII in influenza virus entry via late endosomes. J Virol 77: 460-469.
21. Pleschka S, Jaskunas R, Engelhardt OG, Zurcher T, Palese P, et al. (1996) A plasmid-based reverse genetics system for influenza A virus. J Virol 70: 4188-4192.
22. Ali S, Huber M, Kollewe C, Bischoff SC, Falk W, et al. (2007) IL-1 receptor accessory protein is essential for IL-33-induced activation of T lymphocytes and mast cells. Proc Natl Acad Sci U S A 104: 18660-18665.
23. Mostafa A, Kanrai P, Petersen H, Ibrahim S, Rautenschlein S, et al. (2015) Efficient generation of recombinant influenza A viruses employing a new approach to overcome the genetic instability of HA segments. PLoS One 10:e0116917.
24. Wakai C, Iwama M, Mizumoto K, Nagata K (2011) Recognition of cap structure by influenza B virus RNA polymerase is less dependent on the methyl residue than recognition by influenza A virus polymerase. J Virol 85: 7504-7512.
25. Mazur I, Wurzer WJ, Ehrhardt C, Pleschka S, Puthavathana P, et al. (2007) Acetylsalicylic acid (ASA) blocks influenza virus propagation via its NF-kappaB-inhibiting activity. Cell Microbiol 9: 1683-1694.
26. Bui M, Whittaker G, Helenius A (1996) Effect of M1 protein and low pH on nuclear transport of influenza virus ribonucleoproteins. J Virol 70: 8391-8401.
27. York A, Fodor E (2013) Biogenesis, assembly, and export of viral messenger ribonucleoproteins in the influenza A virus infected cell. RNA Biol 10: 1274-1282.
28. Schmitz ML, Kracht M, Saul VV (2014) The intricate interplay between RNA viruses and NF-kappaB. Biochim Biophys Acta 1843: 2754-2764.
29. Hayashi M, Yamaji Y, Nakazato Y, Saruta T (2000) The effects of calcium channel blockers on nuclear factor kappa B activation in the mesangium cells. Hypertens Res 23: 521-525.
30. Nitsch-Osuch A, Brydak LB (2014) Influenza viruses resistant to neuraminidase inhibitors. Acta Biochim Pol 61: 505-508.
31. Govorkova EA (2013) Consequences of resistance: in vitro fitness, in vivo infectivity, and transmissibility of oseltamivir-resistant influenza A viruses. Influenza Other Respir Viruses 7 Suppl 1: 50-57.
32. Albrecht T, Lee CH, Speelman DJ, Steinsland OS (1987) Inhibition of cytomegalovirus replication by smooth-muscle relaxing agents. Proc Soc Exp Biol Med 186: 41-46.
33. Bolander FF, Blackstone ME, Bradham BM (1990) Cyclic AMP and calcium in mouse mammary tumour virus expression: effects and post-transcriptional site of action. J Mol Endocrinol 5: 27-31.
34. Gazina EV, Harrison DN, Jefferies M, Tan H, Williams D, et al. (2005) Ion transport blockers inhibit human rhinovirus 2 release. Antiviral Res 67: 98-106.
35. Schlesinger MJ, Cahill D (1989) Verapamil and chlorpromazine inhibit the budding of Sindbis and vesicular stomatitis viruses from infected chicken embryo fibroblasts. Virology 168: 187-190.
36. Shainkin-Kestenbaum R, Winikoff Y, Chaimovitz C, Zimlichman S, Sarov I (1993) Inhibitory effect of the calcium antagonist, verapamil, on measles and vaccinia replication in cell culture. Isr J Med Sci 29: 2-6.
37. Gehring G, Rohrmann K, Atenchong N, Mittler E, Becker S, et al. (2014) The clinically approved drugs amiodarone, dronedarone and verapamil inhibit filovirus cell entry. J Antimicrob Chemother 69: 2123-2131.
38. Lavanya M, Cuevas CD, Thomas M, Cherry S, Ross SR (2013) siRNA screen for genes that affect Junin virus entry uncovers voltage-gated calcium channels as a therapeutic target. Sci Transl Med 5: 204ra131.
39. Wurzer WJ, Planz O, Ehrhardt C, Giner M, Silberzahn T, et al. (2003) Caspase 3 activation is essential for efficient influenza virus propagation. EMBO J 22: 2717-2728.
40. Ludwig S, Pleschka S, Planz O, Wolff T (2006) Ringing the alarm bells: signalling and apoptosis in influenza virus infected cells. Cell Microbiol 8: 375-386.